High Temperature Materials & Processes, Vol. 8, No. 2, 113-123

Theoretical Studies on the Concentration Fluctuation in Liquid Alloys: A Liquid Li–Na Alloy as an Example

Kozo Hoshino
Faculty of Engineering, Niigata University, Niigata 950–21, JAPAN

CONTENTS

ABSTRACT

Recent theoretical studies on the structural properties of liquid alloys are reviewed with a special emphasis on the concentration fluctuation. The importance of the concentration-concentration structure factor and the ordering potential is discussed in connection with the ordering character of liquid alloys, e.g. phase-separating and compound-forming alloys.

As a special example, we chose a liquid alloy, $Li_{0.61}Na_{0.39}$, which is a well-known zero alloy with a phase-separating tendency. The structure of the alloy is studied by three approximate theories; the mean-spherical approximation (MSA), the random-phase approximation (RPA) and the hypernetted-chain (HNC) approximation; and by molecular dynamics (MD) simulation. The interatomic potentials are those of the hard-sphere-Yukawa (HSY) model for the MSA calculation and those based on the pseudopotential theory for other calculations. The theoretical results are compared with those of a neutron scattering experiment and it is shown that the theories reproduce well the characteristic features of the experimental results.

1. INTRODUCTION

The structure of liquid alloys has been extensively studied by X-ray, neutron and electron diffraction experiments /1/. They are classified into three types:

I. Simple alloys
The structure of these alloys are well described by hard-sphere (HS) mixture model, since the repulsive interactions between ions play important roles.

II. Phase-separating alloys
These are characterised by a strong clustering tendency and a miscibility gap in their phase diagram. The attractive interaction between like ions is stronger than that between unlike ions. Typical examples are Li-Na and Na-Cs alloys.

III. Compound-forming alloys
These are characterised by a strong chemical short-range order. The strong attractive interaction between unlike ions is important and is taken into account by the Coulomb (or screened Coulomb) interaction in the ionic model /2/ or by the existence of chemical complexes in the compound-forming model /3, 4/. A typical example is Li_4Pb alloy.

There are three types of partial structure factors which have often been used to describe the structure of liquid alloys. They are proposed by Faber and Ziman (FZ) /5/, Ashcroft and Langreth (AL) /6/ and Bhatia and Thornton (BT) /7/. The FZ and AL partial structure factors are related to the density correlation functions between like and unlike chemical species. On the other hand, BT partial structure factors are based on the correlation functions between the number and the concentration. Since the BT partial structure factors contain the concentration as a variable, these are the most convenient partial structure factors for the discussion of the concentration fluctuation in liquid alloys. In fact, they strongly reflect the ordering character of liquid alloys and are also closely related to thermodynamic quantities /8, 9/.

The purpose of the present paper is to review recent theoretical studies on the concentration fluctuation in liquid alloys. The paper is divided as follows: In section 2, the concentration-concentration structure factor is defined and related to the observable quantities. In section 3, the interatomic potentials used are described. The ordering potential is defined and its physical meaning is discussed in section 4. The approximate theoretical methods are described and the results obtained by applying them to the liquid Li-Na alloy are shown in section 5. The results of the computer simulation are shown in section 6. Finally, a summary is given in section 7.

2. CONCENTRATION-CONCENTRATION STRUCTURE FACTOR

Let us consider an alloy A_cB_{1-c} of N_1 atoms of type 1(A) and N_2 atoms of type 2(B) in a total volume V. The total particle number is $N = N_1 + N_2$ and the total particle number density is $n = N/V$. The partial number densities are given by $n_i = N_i/V = c_i n$, where $c_1 = c$ and $c_2 = 1 - c$ are the concentrations.

The BT partial structure factors are defined by:

$$S_{NN}(q) = \frac{1}{N} \langle \Delta n^*(q) \Delta n(q) \rangle , \qquad (1)$$

$$S_{CC}(q) = N \langle \Delta c^*(q) \Delta c(q) \rangle , \qquad (2)$$

$$S_{NC}(q) = \mathrm{Re}\langle \Delta n^*(q)\, \Delta c(q)\rangle, \qquad (3)$$

where $\Delta n(q)$ is the Fourier transform of the local fluctuation, $\Delta n(r) = n(r) - n$, is the total number density and $\Delta c(q)$ is the Fourier transform of the local fluctuation, $\Delta c(r) = c(r) - c$, in the concentration. The brackets $\langle\ \rangle$ and the asterisk stand for the statistical average and the complex conjugate, respectively. The BT partial structure factors are related to the FZ and the AL partial structure factors by the linear transformation (see, e.g. /1/).

The experimentally observable quantity, i.e. the scattering intensity, can be written by the linear combination of the partial structure factors. The coherent neutron scattering intensity I(q), that we are concerned with here, is given by

$$I(q) = \bar{b}^2 S_{NN}(q) + (\Delta b)^2 S_{CC}(q) \qquad (4)$$

$$+ 2\bar{b}(\Delta b) S_{NC}(q)$$

where $\bar{b} = c_1 b_1 + c_2 b_2$, $\Delta b = b_1 - b_2$. The coherent neutron scattering amplitudes are $b_1 - b_2$. Since we have three unknowns, i.e. $S_{NN}(q)$, $S_{CC}(q)$ and $S_{NC}(q)$, we need three independent intensity data to obtain each partial structure factor separately. It is possible, in principle, to do this by using isotopes with different b_i for this purpose. Such isotopes, however, are not always available. Therefore, it is generally difficult to obtain the partial structure factors. It is also possible to separate partial structure factors by combining three different experimental techniques, i.e. X-ray, neutron and electron scatterings. This method is less accurate than the isotope enrichment method, because the scatterers for the neutron, i.e. the nucleus, are different from those for the X-ray and electron, i.e. the electronic charge density. In any case, there exists only a few attempts to obtain the three partial structure factors by these methods. As for other methods, see /1/.

Fortunately, there are special cases, in which we can obtain only the concentration-concentration structure factor $S_{CC}(q)$ from a single neutron scattering measurement. Such alloys are often called 'zero alloy', where $\bar{b} = 0$, and the coherent neutron scattering intensity I(q), given by Eq. (4), is written in this case as

$$I(q) = (\Delta b)^2 S_{CC}(q) \qquad (5)$$

In Fig. 1 we show $S_{CC}(q)$ obtained in such a way for three zero alloys /10/; $Li_{0.61}Na_{0.39}$, $Li_{0.8}Pb_{0.2}$ and $Li_{0.68}Ca_{0.32}$, where $b_i(^7\mathrm{Li}$ isotope) = $-.214 \times 10^{-12}$ cm, $b_{Pb} = .942 \times 10^{-12}$ cm, $b_{Na} = .335 \times 10^{-12}$ cm and $b_{Ca} = .483 \times 10^{-12}$ cm. Since $S_{CC}(q) = c_1 c_2 = c(1 - c)$ for ideal mixtures, we can consider the deviation of $S_{CC}(q)/c_1 c_2$ from unity as the deviation from ideal mixtures. The $S_{CC}(q)$ reflects strongly the ordering character of alloys. The three zero alloys shown in Fig. 1 are typical ones from the viewpoint

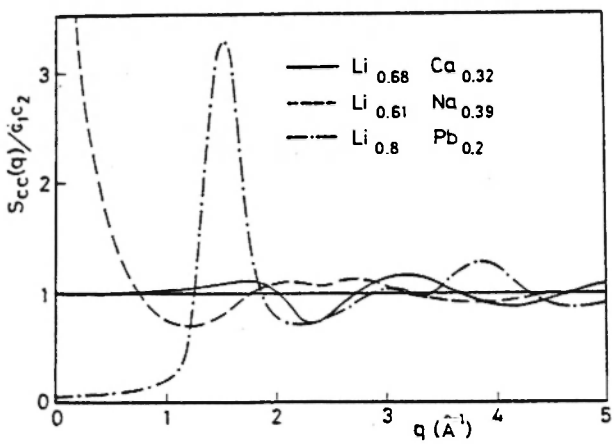

Fig. 1. The concentration-concentration structure factors obtained by the neutron scattering experiments for three zero alloys /10/: $Li_{0.61}Na_{0.39}$, $Li_{0.8}Pb_{0.2}$ and $Li_{0.68}Ca_{0.32}$.

of ordering in alloys; namely, $Li_{0.61}Na_{0.39}$ is the phase-separating alloy, $Li_{0.8}Pb_{0.2}$ the compound-forming alloy and $Li_{0.68}Ca_{0.32}$ the 'ideal' alloy. The characteristic features are as follows: (i) For the phase-separating alloy, $S_{CC}(q)$ shows diverging behaviour in the low q region and its oscillation damps quickly. (ii) For the compound-forming alloy, $S_{CC}(q)$ is small in the low q region and it shows large oscillation, in particular the first peak is very sharp and high. (iii) For the 'ideal' alloy or the simple alloy, $S_{CC}(q) \simeq 1$ for the whole q range.

In the long-wavelength limit, i.e. $q \to 0$, the BT partial structure factors are related to the thermodynamic quantities /7/:

$$S_{NN}(0) = nk_B T\kappa_T + \delta^2 S_{CC}(0) \qquad (6)$$

$$S_{CC}(0) = Nk_B T/(\partial^2 G/\partial c^2)_{P,T,N} \qquad (7)$$

$$= N\langle(\Delta c)^2\rangle$$

$$S_{NC}(0) = -\delta S_{CC}(0) \qquad (8)$$

where

$$\delta = V^{-1}(\partial V/\partial c)_{P,T,N} \quad (9)$$

and G is the Gibbs free energy, κ_T the isothermal compressibility. $S_{CC}(0)$ can be obtained by the electromotive force (EMF) measurement (as for the experimental technique, see /11/),

$$S_{CC}(0) = -(Nk_BT/zF)(1-c)/(\partial E/\partial c)_{T,P} \quad (10)$$

where E is the EMF, F is the Faraday constant and z the valence of the common material in the cell. The EMF measurement is easier than the neutron scattering experiment and, moreover, is *not* restricted to the zero alloy. For this reason, it is possible to obtain $S_{CC}(0)$ as a function of the concentration and we show two examples, Na-Cs /12/ and Li-Pb /13/ alloys, as well as the curve for the ideal mixture in Fig. 2. Since

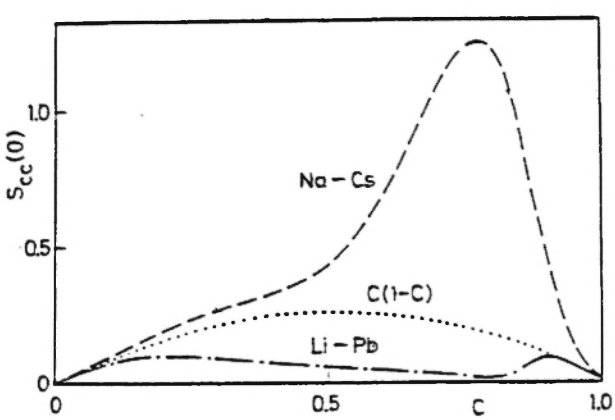

Fig. 2. The long-wavelength limit of the concentration-concentration structure factor $S_{CC}(0)$ as a function of the concentration for the liquid Na-Cs /12/ and Li-Pb /13/ alloys. The dotted curve shows the $S_{CC}(0)$ for the ideal mixture.

$S_{CC}(0) = c(1-c)$ for the ideal mixture, $S_{CC}(0) > c(1-c)$ implies the phase-separating tendency (Na-Cs) and $S_{CC}(0) < c(1-c)$ implies the compound-forming tendency (Li-Pb). Strictly speaking, the Na-Cs alloy does not show phase separation, although it has a strong phase-separating tendency, so that $S_{CC}(0)$ remains finite. On the other hand, the Li-Na alloy shows phase separation and $S_{CC}(q)$ diverges in the long-wavelength limit as is seen from Fig. 1.

3. INTERATOMIC POTENTIALS

In the theoretical treatment of the structure of liquid alloys, the interatomic potentials are the most important basic quantities. The hard-sphere (HS) model has been used to describe the structure of liquid metals and alloys for many years. Though the HS model simulates well the repulsive part of the interatomic potentials, it cannot take account of the attractive part of them. Therefore, the HS model is suitable only for simple liquid metals and alloys and is not satisfactory for describing the structure of non-simple alloys such as phase-separating and compound-forming alloys. In this section we describe the interatomic potentials of the hard-sphere-Yukawa model and those based on the first-principles pseudopotential calculation.

3.1. *Hard-sphere-Yukawa (HSY) Model*

The HSY model is characterised by the interatomic potentials composed of the hard-sphere part and of the Yukawa tail:

$$v_{ij}(r) = \begin{cases} \infty & r < \sigma_{ij} \\ A_{ij}\exp(-\kappa_{ij}r)/r & r > \sigma_{ij} \end{cases} \quad (11)$$

where $\sigma_{ij} = (\sigma_i + \sigma_j)/2$ (σ_i: hard-sphere diameter of i-th component), A_{ij} and κ_{ij} are constants. In Fig. 3, $v_{ij}(r)$ of the HSY model is schematically shown. The Yukawa tail can simulate the attractive or the repulsive interaction by changing the sign of A_{ij}.

In the following we employ the simple HSY model proposed by Waisman /14/, in which the hard-sphere diameter, the number densities and the concentrations of species 1 and 2 are the same, i.e. $\sigma_1 = \sigma_2 = \sigma$, $n_1 = n_2 = n/2$ and $c_1 = c_2 = 1/2$. The interatomic potentials are given by

$$v_{ij}(r) = \begin{cases} \infty & r < \sigma \\ -(-1)^{i+j}A\exp(-\kappa r)/r & r > \sigma \end{cases} \quad (12)$$

where A_{ij} in Eq. (11) is written as $A_{ij} = -(-1)^{i+j}A$ in Eq. (12) and $A > 0$ for the phase-separating alloys.

3.2. *Pseudopotential Theory*

The effective interatomic potentials $v_{ij}(r)$ are given,

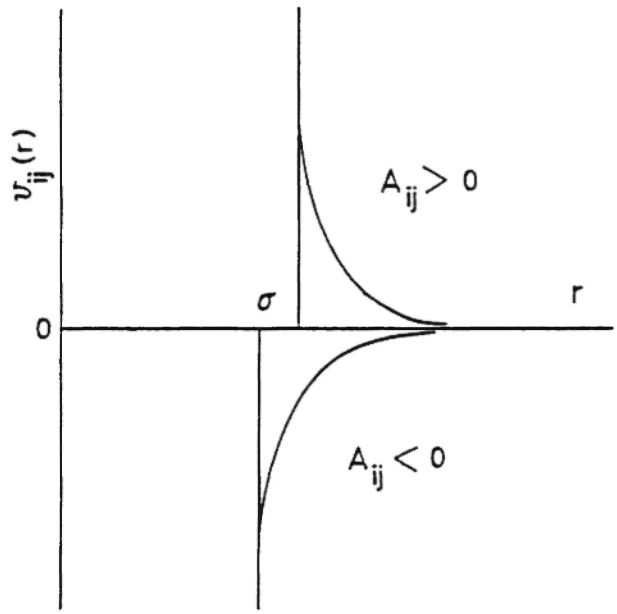

Fig. 3. Schematic illustration of the interatomic potentials of the hard-sphere-Yukawa (HSY) model. The Yukawa tail represents a repulsive (an attractive) potential for $A_{ij} > 0$ ($A_{ij} < 0$).

in the pseudopotential theory, by

$$v_{ij}(r) = z_i z_j e^2/r + 1/(2\pi)^3 \int_0^\infty (q^2/4\pi e^2)\, \tilde{v}_i(q)\, \tilde{v}_j(q) \times (1/\epsilon(q) - 1)(\sin qr/qr)\, 4\pi q^2\, dq\,, \qquad (13)$$

where $\tilde{v}_i(q)$ is the electron-ion pseudopotential, z_i the valence and $\epsilon(q)$ the dielectric function. The first and the second terms in Eq. (13) represent, respectively, the direct Coulomb interactions between ions and the indirect interactions between ions via the conduction electrons. The pseudopotentials and the dielectric function depend on the system; the former depend on the ion and the latter depends on the density of the conduction electrons. Moreover, the dielectric function depends also on the approximation.

When we applied the pseudopotential theory to the liquid Li-Na alloy, we used the Ashcroft potential /15/ for Na,

$$v_{Na}(r) = \begin{cases} 0 & r < r_c \\ -ze^2/r & r > r_c \end{cases} \qquad (14)$$

where the valence z = 1 for Na and r_c is the core radius parameter. This form has been used successfully for describing a variety of properties of Na. On the other hand, we realised that a more realistic pseudopotential for Li was needed because there are only 1s core states and no p core states in Li and therefore, nonlocality is essentially important; i.e. s waves see a different potential from that seen by p waves. For this reason, we /16/ proposed a new pseudopotential for Li,

$$v_{Li}(r) = v_{HXC}(r) + \beta\delta(r) \qquad (15)$$

where $v_{HXC}(r)$ is the full Hartree field corrected for core-valence exchange and correlation in a local density approximation and the second term, having a δ-function form, is applicable to s waves only. Though this is a local potential, it has nonlocality in the sense that s waves see the different potential from other waves, the amplitudes of which vanish at the origin.

In Fig. 4 we show the effective interatomic potentials for $Li_{0.61}Na_{0.39}$ alloy at 590 K. In this calculation we used our pseudopotential for Li, with β = 30 a.u. and the Ashcroft potential for Na with r_c = 1.67 a.u. As for the dielectric function for conduction electron screening, we used the analytic form for local field correction given by Ichimaru and Utsumi /17/.

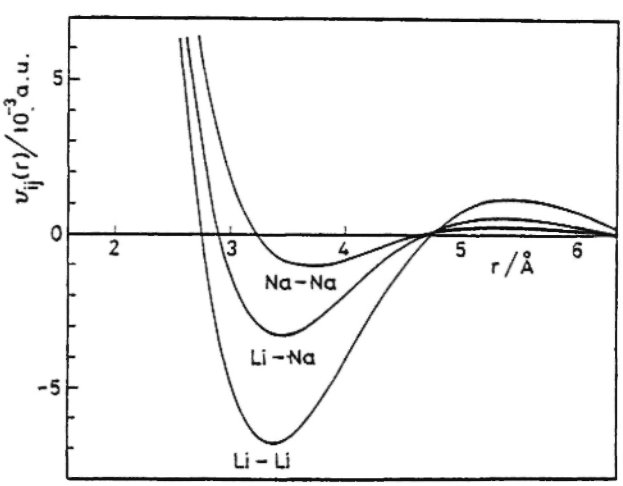

Fig. 4. The effective interatomic potentials, for $Li_{0.61}Na_{0.39}$ alloy at 590 K, obtained by the pseudopotential theory /24/.

4. ORDERING POTENTIAL

Let us define an ordering potential by

$$v_{ord}(r) = v_{12}(r) - [v_{11}(r) + v_{22}(r)]/2 \qquad (16)$$

This quantity is very sensitive to the details of the interatomic potentials and reflects strongly the ordering character of alloys. For phase-separating alloys, $v_{ord}(r) > 0$ around near-neighbour distances. The opposite sign applies for the compound-forming alloys.

Once we obtain the interatomic potentials, we can calculate $v_{ord}(r)$ by Eq. (16). There is another way to obtain $v_{ord}(r)$ approximately from the measured $S_{CC}(q)$. Such an approximate formula was calculated by Copestake *et al.* /2/ by assuming that the number and concentration fluctuations are largely uncoupled, i.e.

$$S_{NC}(q) \ll S_{CC}(q),\ S_{NN}(q) \qquad (17)$$

and that the direct correlation function $c_{ij}(r)$ can be written as

$$c_{ij}(r) = -v_{ij}(r)/k_BT \qquad (18)$$

Equation (18) is correct in a large r region, while Eq. (17) holds for an ionic model, where $S_{NC}(q) = 0$. The approximate formula thus obtained is

$$v_{ord}^{CERS}(r) \simeq (k_BT/16\pi^3 n) \int_0^\infty [1/c_1c_2 - 1/S_{CC}(q)] (\sin qr/qr) 4\pi q^2 dq \qquad (19)$$

Thus, we can obtain $v_{ord}(r)$ theoretically from Eq. (16) by using the interatomic potentials calculated by the pseudopotential theory and also $v_{ord}^{CERS}(r)$ from Eq. (19) by using the experimental $S_{CC}(q)$.

Since the ordering potential depends strongly on the ordering character of alloys, we can use $v_{ord}(r)$ for theoretical studies in the following two ways as illustrated in Fig. 5:

(i) When we start from electronic theory such as the pseudopotential theory, we can calculate $v_{ord}(r)$ from Eq. (16) and compare it with the experimental one. If the agreement is reasonably good, we can be confident that the pseudopotentials used in the calculation and the interatomic potentials are reasonable.

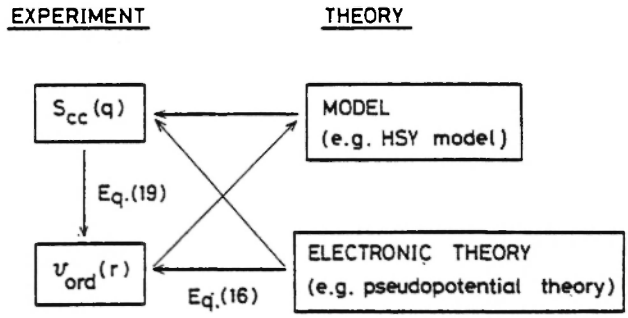

Fig. 5. The two ways of using the ordering potential $v_{ord}(r)$ in the theoretical studies.

Then we further calculate $S_{CC}(q)$ by approximate methods or by computer simulation.

(ii) When we start from a model such as the HSY model, we can determine the parameters in the model by fitting $v_{ord}(r)$ of the model with the experimental one. Then we calculate $S_{CC}(q)$.

In Fig. 6 we compare the theoretical ordering potential derived from the results shown in Fig. 4 with the experimentally based one, derived from Eq. (19) with the experimental $S_{CC}(q)$ /18/, for $Li_{0.61}Na_{0.39}$

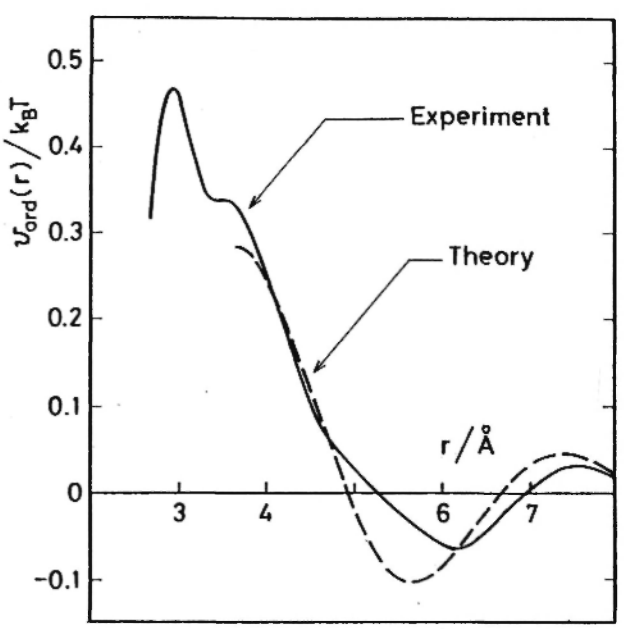

Fig. 6. The theoretical ordering potential, derived from the results shown in Fig. 4, compared with the experimentally based one for $Li_{0.61}Na_{0.39}$ alloy at 590K /27/.

at 590 K. The crucial feature is that both curves are repulsive in the intermediate region around 4 A, which is consistent with the phase-separating tendency. Since the derivation of Eq. (19) is approximate, one cannot expect these results to coincide.

In Fig. 7 we compare the ordering potential based on the HSY model with the experimental one for $Li_{0.61}Na_{0.39}$ at 590 K. The parameters in the HSY model are determined in order to reproduce the 'experimental' $v_{ord}(r)$ around near-neighbour distances. The parameters employed in this calculation are as follows: $\sigma = 2.9$ A, $n = 0.0327\ A^{-3}$, $\eta = \pi n\sigma^3/6 = 0.418$, $z = \kappa\sigma = 3$ and $\theta = \eta A \exp(-\kappa\sigma)/\sigma k_B T = 0.1$ and 0.15.

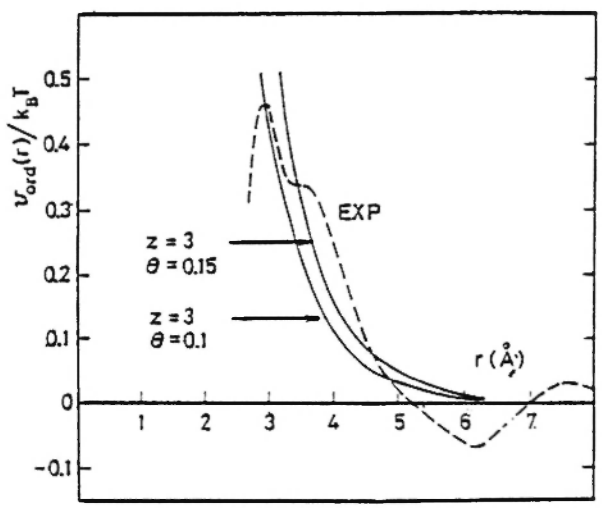

Fig. 7. The ordering potential based on the hard-sphere-Yukawa model compared with the experimental one for $Li_{0.61}Na_{0.39}$ alloy at 590 K /24/. See text for parameters employed.

5. APPROXIMATE THEORIES

When the interatomic potentials $v_{ij}(r)$ are given, there are the following theoretical approaches to calculate the partial structure factors:

(1) Analytic theories
(2) Perturbation theories
(3) Integral-equation theories
(4) Computer simulations

The results obtained by applying (1), (2) and (3) to $Li_{0.61}Na_{0.39}$ are shown in this section and those obtained by (4) are shown in the next section.

5.1. Analytic Theory

The most widely used analytic theory is the mean-spherical approximation (MSA). For the simple HSY model described in section 3.1, Waisman /14/ obtained the analytic solution.

In the MSA, we have the following boundary conditions for the radial distribution function $g_{ij}(r)$ and the direct correlation function $c_{ij}(r)$:

$$g_{ij}(r) = 0 \qquad r < \sigma, \quad (20)$$

$$c_{ij}(r) = -v_{ij}(r)/k_B T$$

$$= (-1)^{i+j}(A/k_B T)\exp(-\kappa r)/r \qquad r > \sigma, \quad (21)$$

By introducing the functions

$$h(r) = [h_{11}(r) + h_{12}(r)]/2 \quad (22)$$

$$\bar{c}(r) = [c_{11}(r) + c_{12}(r)]/2 \quad (23)$$

$$h(r) = [h_{11}(r) - h_{12}(r)]/2 \quad (24)$$

$$c(r) = [c_{11}(r) - c_{12}(r)]/2 \quad (25)$$

where $h_{ij}(r) = g_{ij}(r) - 1$, Waisman showed that the equations for $h(r)$ and $\bar{c}(r)$ are the same as the Percus-Yevick ones for a pure hard-sphere fluid of diameter σ at number density n. These analytic forms follow, therefore, from the work of Wertheim /19/ and Thiele /20/. On the other hand, the equations for $h(r)$ and $c(r)$ are given by

$$h(r) = 0 \qquad r < \sigma \quad (26)$$

$$c(r) = (A/k_B T)\exp(-\kappa r)/r \qquad r > \sigma \quad (27)$$

and

$$h(r) = c(r) + n\int h(r')c(|\underset{\sim}{r} - \underset{\sim}{r}'|)\,d\underset{\sim}{r}' \quad (28)$$

Waisman formulated the analytic solution of Eqs. (26), (27) and (28).

In Fig. 8 we compare $S_{CC}(q)/c_1c_2$ obtained by the MSA to that of the neutron diffraction experiment for $Li_{0.61}Na_{0.39}$ at 590 K. In this calculation we /21/ employed the same parameters as those used in Fig. 7. We see that the characteristic features of

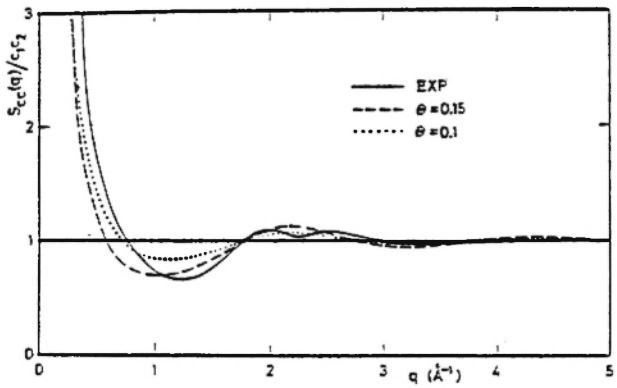

Fig. 8. Concentration–concentration structure factors of the hard-sphere–Yukawa model in the MSA compared with the experimental one /18/ (full curve) for liquid $Li_{0.61}Na_{0.39}$ alloy at 590 K /21/. The MSA results are shown for θ = 0.1 (dotted curve) and θ = 0.15 (broken curve), corresponding to the two curves for the ordering potentials in Fig. 7.

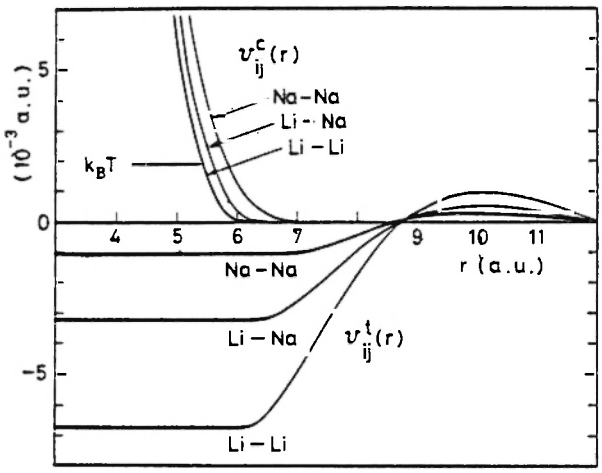

Fig. 9. The WCA decomposition of the interatomic potentials shown in Fig. 4 into core and tail parts /24/.

the experimental $S_{CC}(q)$ are well reproduced by the HSY model in the MSA.

5.2. *Perturbation Theory*

There are many kinds of perturbation theories (see /8/) but the random-phase approximation (RPA) is the simplest of them. In the RPA we treat the tail part of the interatomic potentials perturbationally. First, we split the interatomic potentials, in the spirit of WCA /22/, into core and tail parts defined, respectively, by

$$v_{ij}^c(r) = \begin{cases} v_{ij}(r) - v_{ij}(r_{ij}^0) & r < r_{ij}^0 \\ 0 & r > r_{ij}^0 \end{cases} \quad (29)$$

and

$$v_{ij}^t(r) = \begin{cases} v_{ij}(r_{ij}^0) & r < r_{ij}^0 \\ v_{ij}(r) & r > r_{ij}^0 \end{cases} \quad (30)$$

where r_j^0 is the position of the principal minimum of $v_{ij}(r)$, i.e.

$$v_{ij}^{min} = v_{ij}(r_{ij}^0) \quad (31)$$

In Fig. 9 we illustrate $v_{ij}^c(r)$ and $v_{ij}^t(r)$ obtained in this way from $v_{ij}(r)$ of Fig. 4. Next, we replace the core parts by the hard sphere model. The effective hard-sphere diameters σ_{ij}^{eff} are determined using relation /23/

$$v_{ij}(\sigma_{ij}^{eff}) - v_{ij}^{min} = k_BT \quad (32)$$

Then, in the RPA, the direct correlation functions are written as

$$c_{ij}(r) = c_{ij}^{HS}(r) - v_{ij}^t(r)/k_BT \quad (33)$$

where $c_{ij}^{HS}(r)$ are the direct correlation functions of the hard-sphere mixture with the effective hard-sphere diameters obtained by Eq. (32). Once we know the $c_{ij}(r)$, it is straightforward to calculate the partial structure factors. We show $S_{CC}(q)/c_1c_2$ determined in this way in Fig. 10. There are two regions of failure of the RPA, one very close to the origin and the other around 2.2 Å^{-1}. This breakdown of the RPA is caused mainly by the strong attractive tail in $v_{LiLi}(r)$. For further details, see /24/.

5.3. *Integral-equation Theory*

The well-known integral-equation theories are the hypernetted-chain (HNC) and the Percus-Yevick (PY) approximations /25/. In the HNC approximation, the equations

$$c_{ij}(r) = h_{ij}(r) - \ln[h_{ij}(r) + 1] - v_{ij}(r)/k_BT \quad (34)$$

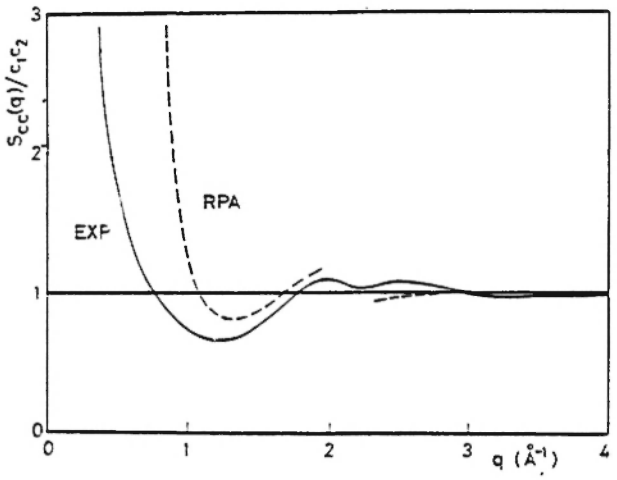

Fig. 10. Concentration-concentration structure factors calculated in the RPA (broken curve) compared with experimental results /18/ (full curve) for liquid $Li_{0.61}Na_{0.39}$ alloy at 590 K /24/.

together with the Ornstein-Zernike relation

$$h_{ij}(r) = c_{ij}(r) + \sum_k n_k \int h_{ik}(r')\, c_{kj}(|\underset{\sim}{r} - \underset{\sim}{r}'|)\, d\underset{\sim}{r}' \qquad (35)$$

must be solved. We used Gillan's algorithm /26/ to solve these equations numerically. In Fig. 11 the HNC result /27, 28/ of $S_{CC}(q)/c_1c_2$ is compared with the experimental one. The agreement is substantial, particularly for $q < 2A^{-1}$. Over this range, the theory reproduces quite well the divergence around the origin as well as, in shape, size and position, the minimum at $q = 1.2A^{-1}$. In Fig. 12 we /28/ show $S_{NN}(q)$, $S_{CC}(q)$ and $S_{NC}(q)$. It should be noted that $S_{NC}(q)$ is quite small over the whole range. Therefore, the assumption employed by Copestake *et al.* mentioned in section 4 is shown to be reasonable for this Li-Na alloy.

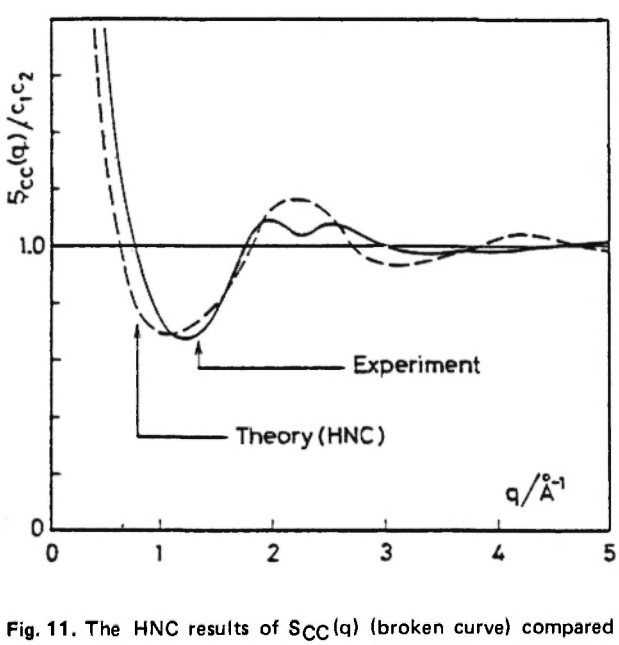

Fig. 11. The HNC results of $S_{CC}(q)$ (broken curve) compared with the experimental one /18/ (full curve) for the liquid $Li_{0.61}Na_{0.39}$ alloy at 590 K /27, 28/.

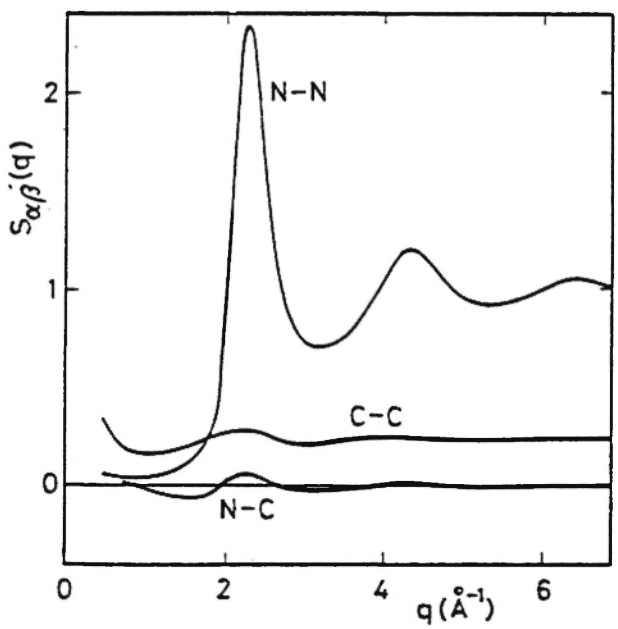

Fig. 12. Partial structure factors, $S_{NN}(q)$, $S_{CC}(q)$ and $S_{NC}(q)$, obtained by the HNC calculation for liquid $Li_{0.61}Na_{0.39}$ alloy at 590 K /28/.

6. COMPUTER SIMULATION

Recently, two computer simulations, the molecular dynamics and the Monte Carlo methods, have been extensively used to study the structure of liquid metals and alloys. We /29/ have employed the molecular dynamics (MD) method, where the interatomic potentials acquired from the pseudopotential theory are input data. Although no approximation is involved in the molecular dynamics calculation, the accuracy is limited by the effects of the finite size of the system. The parameters used in our MD simulation for $Li_{0.61}Na_{0.39}$ are as follows: the total number of atoms N = 256 (156 Li and 100 Na atoms); the system is a cube

L x L x L, where L ≒ 20 A, and the periodic boundary condition is employed; the interatomic potentials are the same as those shown in Fig. 4 and the force range is L/2 ≒ 10 A; the temperature is 590 K.

In Fig. 13 we show the partial radial distribution functions $g_{ij}(r)$. Since the system used in the MD simulation is a cube with L ≒ 20 A, the $g_{ij}(r)$ are available for $r < L/2 \doteq 10$A. It can be seen that the first peaks of $g_{LiLi}(r)$ and $g_{NaNa}(r)$ are higher than that of $g_{LiNa}(r)$, which suggests that homo-coordination is dominant in this system. This is a characteristic feature of a phase-separating system. Note that, for hetero-coordinating systems such as molten salts, the first peak of $g_{ij}(r)$ for unlike pairs is higher than that for the like pairs; see e.g. Edwards *et al.* /30/ for molten NaCl.

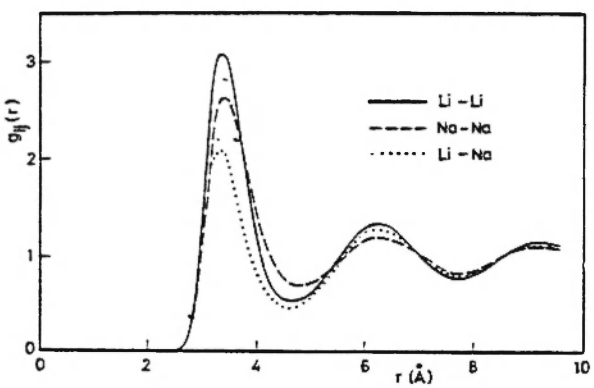

Fig. 13. Partial radial distribution functions obtained by the molecular dynamics simulation for liquid $Li_{0.61}Na_{0.39}$ alloy at 590 K /29/.

In Fig. 14 we show the partial structure factors $S_{CC}(q)/c_1c_2$, $S_{NN}(q)$ and $S_{NC}(q)$ obtained from $g_{ij}(r)$ by the Fourier transformation. The characteristic features of the partial structure factors are the same as those of HNC: $S_{CC}(q)$ diverges in the low q region and has a minimum around $q \doteq 1.2\,A^{-1}$; $S_{NN}(q)$ has a sharp first peak at $q \cong 2.2\,A^{-1}$; $S_{NC}(q)$ is very small throughout. It should be noted that information about the partial structure factors for $q < \pi/(L/2) \cong 0.3A^{-1}$ is not attainable, in principle, by the Fourier transform of the $g_{ij}(r)$ determined by MD, because $g_{ij}(r)$ are only available for $0 < r < L/2$ in the MD simulation.

Finally, in Fig. 15 we compare $S_{CC}(q)/c_1c_2$ derived from the $g_{ij}(r)$ obtained by MD with those of HNC and experiment. These three results agree reasonably with each other. Since we used the same interatomic potentials for the MD and the HNC calculations, the difference between the MD and the HNC results measures the accuracy of the HNC approximation. We have to be careful, however, because the $S_{CC}(q)$ is not directly attainable by the MD simulation. As already indicated, we need Fourier transform of the $g_{ij}(r)$, which are available only in the finite range. Therefore $S_{CC}(q)$ is less accurate than $g_{ij}(r)$ in the

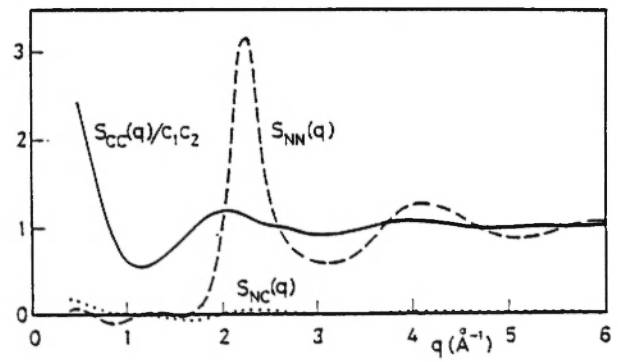

Fig. 14. Partial structure factors $S_{CC}(q)/c_1c_2$, $S_{NN}(q)$ and $S_{NC}(q)$ derived, by the Fourier transformation, from the $g_{ij}(r)$ shown in Fig. 13 /29/.

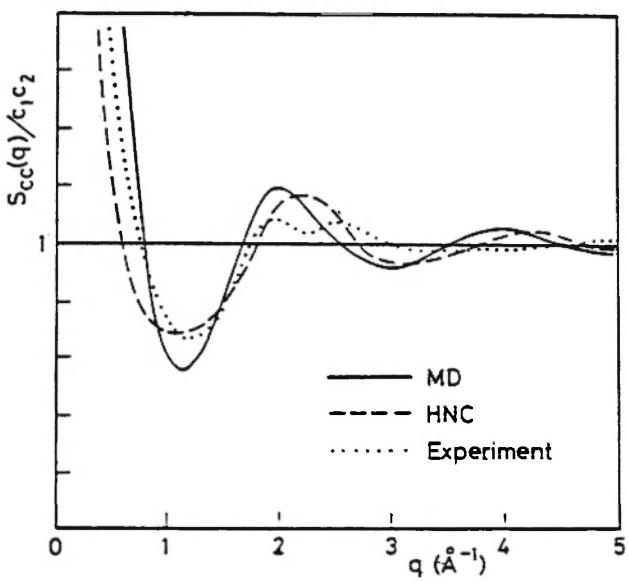

Fig. 15. Concentration-concentration structure factors for liquid $Li_{0.61}Na_{0.39}$ alloy at 590 K. The molecular dynamics result (Fig. 14) is compared with that of the HNC result /27, 28/ shown in Fig. 11 and with the experimental one /18/.

MD calculation. Moreover, we are working with a finite system, where N = 256, so that our MD results are not 'exact' for this reason also.

7. SUMMARY

Recent theoretical studies on the structure of liquid alloys are briefly reviewed in connection with an example of a phase-separating Li-Na alloy. In sections 2, 3 and 4, the importance of the concentration-concentration structure factor, the interatomic potentials and the ordering potentials is emphasised in relation to the ordering character of alloys. In section 5, three typical approximate theories, MSA, RPA, and HNC, are applied to liquid $Li_{0.61}Na_{0.39}$ alloy and the results are compared with an experimental one. Finally, in section 6, molecular dynamics simulation is used to study the structural properties of the liquid $Li_{0.61}Na_{0.39}$ alloy. It is demonstrated that the theoretical results for $S_{CC}(q)$ obtained in sections 5 and 6 agree reasonably well with the experimental measurements.

Although only one specific example, liquid $Li_{0.61}Na_{0.39}$ alloy, is discussed in this paper, the theoretical concepts and the methods described can be used, of course, for understanding the structural properties of other liquid alloys.

ACKNOWLEDGEMENTS

The author would like to thank Professor W.H. Young for numerous useful discussions. Most of the theoretical results shown in this paper are based on works studied in collaboration with Professor Young.

REFERENCES

1. WASEDA Y., The Structure of Non-Crystalline Materials, Liquids and Amorphous Solids, McGraw-Hill, New York (1980).
2. COPESTAKE, A.P., EVANS, R., RUPPERSBERG, H. and SCHIRMACHER, W., *J. Phys. F: Metal Phys.*, **13**, 1993 (1983).
3. BHATIA, A.B., HARGROVE, W.H. and THORNTON, D.E., *Phys. Rev.*, **B9**, 435 (1974); BHATIA, A.B. and HARGROVE, W.H., *Phys. Rev.*, **B10**, 3186 (1974).
4. HOSHINO, K. and YOUNG, W.H., *J. Phys. F: Metal Phys.*, **10**, 1365 (1980).
5. FABER, T.E. and ZIMAN, J.M., *Phil. Mag.*, **11**, 153 (1965).
6. ASHCROFT, N.W. and LANGRETH, D.C., *Phys. Rev.*, **156**, 500 (1967).
7. BHATIA, A.B. and THORNTON, D.E., *Phys. Rev.*, **B2**, 3004 (1970).
8. YOUNG, W.H., *Can. J. Phys.*, **65**, 241 (1987).
9. TAMAKI, S., in Proc. Sixth Int. Conf. Liquid and Amorphous Metals, *Z. fur Phys. Chem.*, **156**, 537 (1988); WASEDA, Y., JACOB, K.T. and TAMAKI, S., *High Temp. Mater. Proc.*, **6**, 119 (1984).
10. CHIEUX, P. and RUPPERSBERG, H., *J. Physique*, **C8**, **41**, 145 (1980); YOUNG, W.H., in Proc. Third Int. Conf. Structure of Non-Crystalline Materials, *J. Physique*, **C8**, 427 (1985).
11. TAMAKI, S. and CUSACK, N.E., *J. Phys. F: Metal Phys.*, **9**, 403 (1979).
12. NEALE, F.E. and CUSACK, N.E., *J. Phys. F: Metal Phys.*, **12**, 2839 (1982).
13. SABOUNGI, M.L., MARR, M. and BLANDER, M., *J. Chem. Phys.*, **68**, 1375 (1978).
14. WAISMAN, E., *J. Chem. Phys.*, **59**, 495 (1973).
15. ASHCROFT, N.W., *Phys. Lett.*, **23A**, 48 (1966).
16. HOSHINO, K. and YOUNG, W.H., *J. Phys. F: Metal Phys.*, **16**, 1659 (1986).
17. ICHIMARU, S. and UTSUMI, K., *Phys. Rev.*, **B24**, 7385 (1981).
18. RUPPERSBERG, H. and KNOLL, W., *Z. Naturf.*, **a32**, 1374 (1977).
19. WERTHEIM, M.S., *Phys. Rev. Lett.*, **10**, 321 (1963).
20. THIELE, E., *J. Chem. Phys.*, **38**, 1959 (1963).
21. HOSHINO, K. and YOUNG, W.H., *J. Phys. F: Metal Phys.*, **16**, L73 (1986).
22. WEEKS, J.D., CHANDLER, D. and ANDERSEN, H.C., *J. Chem. Phys.*, **54**, 5237 (1971); **55**, 5422 (1971).
23. MEYER, A., SILBERT, M. and YOUNG, W.H., *Phys. Chem. Liq.*, **10**, 279 (1981); **13**, 293 (1984).
24. HOSHINO, K. and YOUNG, W.H., *J. Phys. F: Metal Phys.*, **16**, 1671 (1986).
25. HANSEN, J.P. and McDonald, I.R., Theory of Simple Liquids, Academic Press (1976).
26. GILLAN, M.J., *Mol. Phys.*, **38**, 1781 (1979); ABERNETHY, G.M. and GILLAN, M.J., *Mol. Phys.*, **39**, 839 (1980).
27. HOSHINO, K. and YOUNG, W.H., in Proc. Sixth Int. Conf. Liquid and Amorphous Metals, *Z. fur Phys. Chem.*, **156**, 651 (1988).
28. HOSHINO, K., SILBERT, M., STAFFORD, A. and YOUNG, W.H., *J. Phys. F: Metal Phys.*, **17**, L49 (1987).
29. HOSHINO, K. and VAN WERING, J.J., *J. Phys. F: Metal Phys.*, **18**, L23 (1988).
30. EDWARDS, F.G., ENDERBY, J.E., HOWE, R.A. and PAGE, D.I., *J. Phys. C: Solid St. Phys.*, **8**, 3483 (1975).